Strongly interacting singlet-doublet Higgs model

A. Hill
University of Michigan, Department of Physics, Ann Arbor, Michigan 48109

J. J. van der Bij
Fermi National Accelerator Laboratory, P.O. Box 500, Batavia, Illinois 60510

(Received 17 February 1987)

We study the effects on the vector-boson parameters due to a heavy scalar singlet interacting strongly with the Higgs sector of the standard model. The one-loop-induced effects due to the additional scalar are not suppressed by inverse powers of its mass. In the limit that the singlet-Higgs coupling becomes much larger than the Higgs self-coupling, the $4W$ vertex differs from that in the standard model. In this limit the leading corrections are not related to the divergences of the gauged nonlinear σ model.

I. INTRODUCTION

It is now known for certain that the weak interactions are mediated by massive vector bosons. Because the theory of massive vector bosons is not renormalizable, one postulates in the standard model the existence of an additional scalar field: the Higgs boson. This extra particle makes the model renormalizable. Since evidence of the Higgs particle has not been found so far, it is natural to study the standard model in the limit that the Higgs-boson mass becomes very large.[1,3-7] In this limit the Higgs sector becomes strongly interacting and, therefore, the decoupling theorem[2] is not applicable. As a result, the low-energy effective Lagrangian for the vector bosons contains terms that grow with the Higgs-boson mass.[3] In order to discuss the possible effects, it is useful to describe both the standard model and the effective theory in a gauge-invariant way.

The standard model is a gauged linear σ model:[4]

$$\mathcal{L}=-\tfrac{1}{2}(D_\mu\Phi)^\dagger(D^\mu\Phi)-\frac{\lambda}{8}(\Phi^\dagger\Phi-f^2)^2 , \tag{1.1}$$

$$\Phi=(\sigma+i\boldsymbol{\tau}\cdot\boldsymbol{\phi})\begin{bmatrix}1\\0\end{bmatrix} . \tag{1.2}$$

At the tree level, the Higgs particle can be removed from (1.1) by taking the limit $\lambda\to\infty$ or, equivalently, $m_H{}^2\to\infty$. The standard model then turns into a gauged nonlinear σ model

$$\mathcal{L}=-\frac{f^2}{4}\mathrm{Tr}(D_\mu U)^\dagger(D^\mu U) , \tag{1.3}$$

$$U=\sqrt{1-\boldsymbol{\pi}^2}+i\boldsymbol{\tau}\cdot\boldsymbol{\pi},\quad \boldsymbol{\pi}=\frac{\boldsymbol{\phi}}{f} \tag{1.4}$$

which is equivalent to massive Yang-Mills theory. That the standard model has the limit (1.3) can be see on a formal level by noting that for a finite energy density $\Phi^\dagger\Phi\to f^2$ as $\lambda\to\infty$. In the language of diagrams, the sum of all light-particle-irreducible (LPI) contributions from (1.1), with only external ϕ lines, converges to the corresponding term in the expansion of (1.3) for small $\boldsymbol{\phi}^2/f^2$.

At the one-loop level it is found[5] that the effective interactions induced by the heavy Higgs particle can be described by higher-order covariant-derivative terms of U; in the unitary gauge these terms correspond to extra interactions of the vector bosons beyond the ordinary gauge couplings. The corrections to vector-boson parameters grow only logarithmically with the Higgs-boson mass. The corrections can be found in two ways. The first is to calculate in the linear model (1.1) keeping only terms of $O(\ln m_H{}^2)$. The second method is the calculation of the logarithmic divergences in the nonlinear model (1.3) using dimensional regularization. A comparison of the two calculations gives the following correspondence: The coefficients of the nonrenormalizable logarithmic divergences of the gauged nonlinear σ model (poles in $n-4$) describe correctly the effects of a heavy Higgs particle on low-energy physics. The exact correspondence is[3]

$$\text{linear model: } \ln m_H{}^2 \leftrightarrow \text{nonlinear model: } -\frac{2}{n-4} . \tag{1.5}$$

Explicit two-loop calculations[6] indicate that there is no simple relation between these models at that level. This is at least partly due to the presence of the Higgs self-coupling in the two-loop diagrams; at the one-loop level the diagrams that contain a Higgs self-coupling either cancel or the λ dependence of a vertex cancels that of a propagator.

One can, therefore, ask whether a relation such as Eq. (1.5) will hold in more general Higgs models as well. One would normally expect the only requirement to be that the model have (1.3) as its limit when the Higgs-boson mass becomes large. It is already known that (1.5) is independent of the exact form of the Higgs potential if no more than one Higgs particle is present. The next simplest model one can consider is the addition of a singlet particle which only interacts with the Higgs sector of the standard model. Because the singlet does not couple directly to vector bosons, one would expect (1.5) to be unchanged. In particular, the decoupling theorem

seems to indicate that contributions of such a particle would be suppressed by inverse powers of its mass. However the possibility of Higgs-singlet mixing complicates the situation and thus only an explicit calculation can settle this question. The purpose of the present paper is to study such a model. The quantum corrections to the ρ parameter, the $3W$ vertex and the $4W$ vertex are calculated. They are then compared to the corresponding corrections obtained in the standard model without the additional singlet field.

The model is described in Sec. II and it is shown to be renormalizable in Sec. III. Sections IV, V, and VI are devoted to the calculation of the one-loop corrections to the ρ parameter, the $3W$ vertex, and the $4W$ vertex, respectively. A discussion of the results follows in Sec. VII.

II. THE MODEL

The fundamental gauge-invariant building block of the Higgs sector is $\Phi^\dagger\Phi$. Therefore, the simplest coupling of a particle to the Higgs fields is

$$\tilde{\lambda} x \Phi^\dagger \Phi \ , \tag{2.1}$$

where x is a scalar field. In an unbroken theory the corrections due to an interaction of this kind would be suppressed by factors of $m_x{}^{-2}$, according to the decoupling theorem.[2] In the broken case, however, the Higgs field develops a vacuum expectation value and, after shifting it, the vertex (2.1) leads to mixing between the scalar and the Higgs. This can give rise to new effects even in diagrams that do not involve the scalar explicitly.

The simplest Lagrangian which incorporates the vertex (2.1) is

$$\mathcal{L} = -\tfrac{1}{2}(D_\mu\Phi)^\dagger(D^\mu\Phi) - \tfrac{1}{2}(\partial_\mu x)^2 - \frac{\lambda_1}{8}(\Phi^\dagger\Phi - f_1{}^2)^2 - \frac{\lambda_2}{8}(2f_2 x - \Phi^\dagger\Phi)^2 + \mathcal{L}_{\text{gauge}} \ , \tag{2.2}$$

where f_1 is the vacuum expectation value of the Higgs field, which is related to the vector-boson mass M_W through

$$M_W = \frac{g f_1}{2} \ , \tag{2.3}$$

and x is a scalar under all transformations. It is evident from (2.2) that, in the limit $\lambda_1 \to \infty$, the model (2.2) reduces to the nonlinear model (1.3) and a free field x. Note that this argument is independent of the strength of the new coupling λ_2; again, as in the simple model, the sum of all LPI tree graphs converges to the appropriate term in the expansion of (1.3), as can be verified by explicit calculation.

The potential of the extended model can also be written as

$$\mathcal{V} = \frac{\lambda_2}{8}(2f_2 x - f_1{}^2)^2 - \frac{\lambda_2}{4}(2f_2 x - f_1{}^2)(\Phi^\dagger\Phi - f_1{}^2) + \frac{\lambda_3}{8}(\Phi^\dagger\Phi - f_1{}^2)^2 \ , \tag{2.4}$$

$$\lambda_3 = \lambda_1 + \lambda_2 \ . \tag{2.5}$$

Therefore, both x and σ develop a vacuum expectation value. The Higgs self-coupling is replaced by λ_3 which changes the relation between the coupling constant and the Higgs-boson mass (cutoff parameter). The eigenvalues of the mass matrix are

$$m_\pm{}^2 = \tfrac{1}{2}(\lambda_2 f_2{}^2 + \lambda_3 f_1{}^2) \pm [\lambda_2{}^2 f_1{}^2 f_2{}^2 + \tfrac{1}{4}(\lambda_2 f_2{}^2 - \lambda_3 f_1{}^2)^2]^{1/2} \ , \tag{2.6}$$

and the Higgs propagator changes to

$$\sigma - \sigma: \quad ------ = \frac{\alpha}{k^2 + m_+{}^2} + \frac{1-\alpha}{k^2 + m_-{}^2} \ , \tag{2.7}$$

the mixed propagator

$$x - \sigma: \quad ——— = \gamma \left[\frac{1}{k^2 + m_-{}^2} - \frac{1}{k^2 + m_+{}^2} \right] \ , \tag{2.8}$$

and the x propagator

$$x - x: \quad ——— = \frac{1-\alpha}{k^2 + m_+{}^2} + \frac{\alpha}{k^2 + m_-{}^2} \ , \tag{2.9}$$

where

$$\alpha = \frac{m_+{}^2 - \lambda_2 f_2{}^2}{m_+{}^2 - m_-{}^2} \tag{2.10}$$

and

$$\gamma = \frac{\lambda_2 f_1 f_2}{m_+{}^2 - m_-{}^2} \ . \tag{2.11}$$

Note that $0 \le \alpha \le 1$.

The Feynman rules that deviate from those of the standard model are listed in Table I. In all calculations it was assumed that both masses $m_\pm{}^2$ are large compared to the W mass. This is the relevant limit for studying the effects of heavy particles on low-energy

TABLE I. New vertices in the extended lagrangian.

σ-σ	------	$= \dfrac{\alpha}{k^2 + m_+{}^2} + \dfrac{1-\alpha}{k^2 + m_-{}^2}$
x-σ	———	$= \gamma \left[\dfrac{1}{k^2 + m_+{}^2} - \dfrac{1}{k^2 + m_-{}^2} \right]$
x-x	———	$= \dfrac{1-\alpha}{k^2 + m_+{}^2} + \dfrac{\alpha}{k^2 + m_-{}^2}$
	$\overset{a}{\underset{b}{\prec}} = \lambda_2 f_2 \delta_{ab}$	$-\!\!\prec = \lambda_2 f_2$

TABLE II. The effective vertices.

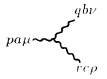	$=ig\epsilon_{abc}(\delta g+\frac{3}{2}Z_W+\alpha_3 g^2)[(p-q)_\rho\delta_{\mu\nu}+(r-p)_\nu\delta_{\mu\rho}+(q-r)_\mu\delta_{\nu\rho}]$
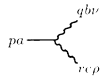	$=2\alpha_3 g^2\epsilon_{abc}[\delta_{\nu\rho}p\,(q-r)+q_\nu q_\rho-r_\nu r_\rho]$
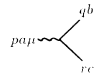	$=4i\alpha_3 g\,\epsilon_{abc}(pqr_\mu-prq_\mu)+O(p,q,r)$
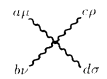	$=[-2g^2(\delta g+Z_W+\alpha_3 g^2)(2\delta_{\mu\nu}\delta_{\rho\sigma}-\delta_{\mu\rho}\delta_{\nu\sigma}-\delta_{\mu\sigma}\delta_{\nu\rho})$ $+2\alpha_1 g^4\delta_{\mu\nu}\delta_{\rho\sigma}+\alpha_2 g^4(\delta_{\mu\rho}\delta_{\nu\sigma}+\delta_{\mu\sigma}\delta_{\nu\rho})]\delta_{ab}\delta_{cd}+$ permutations
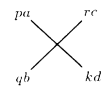	$=\{8\alpha_1[-s(t+u)+(p^2+q^2)(r^2+k^2)]$ $+4\alpha_2[-2ut-s(t+u)+2(p^2q^2+r^2k^2)+(p^2+q^2)(r^2+k^2)]\}\delta_{ab}\delta_{cd}$ $+$ permutations

physics; i.e., in this limit the question of decoupling can be investigated.

One could just as well write the Lagrangian (2.2) in terms of the diagonalized fields $\bar{x}$ and $\bar{\sigma}$. They would then both couple to the vector bosons. This obscures, however, the scalar nature of x; in other words, the finiteness to all orders of xW vertices is not obvious. Consequently the analysis of the $3W$ and particularly the $4W$ vertex becomes more complicated.

With the exception of $\delta\rho$, for the purpose of this paper it is sufficient to investigate only the SU(2) model since the inclusion of the U(1) group would merely complicate the α_i (Ref. 7) [see Eq. (2.13) below] without altering the main conclusion. The covariant derivative in Eq. (2.2) is then

$$D_\mu\Phi=\left[\partial_\mu-\frac{ig}{2}\mathbf{W}_\mu\cdot\boldsymbol{\tau}\right]\Phi\ . \tag{2.12}$$

All calculations were performed in the Feynman gauge.

In the SU(2) model, the logarithmic effects of a strongly interacting Higgs sector can be summarized by the effective Lagrangian of Appelquist and Bernard:[5]

$$\begin{aligned}\mathcal{L}_{\text{eff}}=&\alpha_0\mathcal{L}_0+\alpha_1\mathrm{Tr}(V_\mu V^\mu)\mathrm{Tr}(V_\nu V^\nu)\\&+\alpha_2\mathrm{Tr}(V_\mu V^\nu)\mathrm{Tr}(V_\nu V^\mu)\\&+g\alpha_3\mathrm{Tr}(F_{\mu\nu}[V^\mu,V^\nu])\\&+\alpha_4\mathrm{Tr}(D_\mu V^\mu D_\nu V^\nu)\ ,\end{aligned} \tag{2.13}$$

where

$$V_\mu=(D_\mu U)U^\dagger \tag{2.14}$$

and

$$F_{\mu\nu}=\left[\partial_\mu-\frac{ig}{2}\mathbf{W}_\mu\cdot\boldsymbol{\tau}\right]\frac{\mathbf{W}_\nu\cdot\boldsymbol{\tau}}{2i}-(\mu\leftrightarrow\nu)\ . \tag{2.15}$$

These coefficients are determined by comparing the result of the one-loop calculations with the Feynman rules which follow from (2.13). That this can be done is a consequence of the fact that (2.2) reproduces the nonlinear σ model in the limit $\lambda_1\to\infty$. The rules for the required terms in the expansion of (2.13) for small π fields are shown in Table II.

Since the structure of (2.13) is the same for the simple and the extended model, differences can only appear in the coefficients α_i. As in the standard model, the structure α_4 turns out not to have a logarithmic divergence and will therefore be omitted from the following.

III. RENORMALIZABILITY

A simple power-counting argument establishes that the Lagrangian (2.2) is indeed renormalizable even without x self-couplings. The scalar appears only in three-point vertices and then only linearly.

The superficial degree of divergence of a diagram is given by

$$D=nL-2I+\partial\ , \tag{3.1}$$

$$L=I-V+1\ , \tag{3.2}$$

TABLE III. Degree of divergence for vertices absent from Eq. (2.2).

Vertex	x^3	x^4	$x^2\sigma$	$x^3\sigma$	$x^2(\sigma^2+\phi^2)$	$x\sigma(\sigma^2+\phi^2)$	$x\sigma W^2$	xW^2	x^2W^2
$D\leq$	-2	-4	-1	-3	-2	-1	-1	0	-2

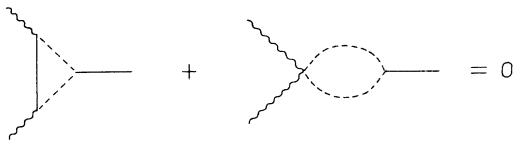

FIG. 1. Cancellation of contributions to the xW^2 vertex.

where n L, I, V, and ∂ are the number of dimensions, loops, internal lines, vertices and derivatives in vertices, respectively.

The Lagrangian can symbolically be written as

$$\begin{aligned}\mathcal{L}=&a_1x(\sigma^2+\phi^2)+a_2\sigma(\sigma^2+\phi^2)\\&+a_3\sigma W^2+a_4\partial\sigma\phi W+a_5\partial\phi^2W\\&+a_6\partial W^3+a_7(\sigma^2+\phi^2)^2\\&+a_8W^2(\sigma^2+\phi^2)+a_9W^4\ .\end{aligned}\tag{3.3}$$

With the usual relations among the above quantities and

$$V_1=E_x+2I_x+I_{x\sigma}\ ,\tag{3.4}$$

which follows from the fact that each vertex a_1 contains exactly one x line, D can be expressed as

$$D=4-V_2-V_3-2I_x-I_{x\sigma}-2E_x-E_\sigma-E_\phi-E_W\ .\tag{3.5}$$

The degree of divergence D for the dimension-3 and -4 vertices that do not appear in (2.2) is listed in Table III; note that, since x is a singlet, all gauge-invariant vertices involving only x and W fields are of dimension 5 and higher and are therefore not divergent. The two diagrams, which contribute to the xW^2 vertex in leading order, cancel (see Fig. 1). Note that $D=0$ for this vertex, so that only gauge invariance ensures the renormalizability of the Lagrangian (2.2) without this term. This is similar to the cancellation of the fermion loops that contribute to the ${A_\mu}^4$ vertex in QED. There is also a $D=2$ tadpole term in x which, however, has no physical effects.

IV. CORRECTIONS TO THE ρ PARAMETER

It can be shown that the Higgs-boson-mass dependent contribution to $\delta\rho$ only arises from the diagram in Fig. 2; note that it is logarithmically divergent and contains one Higgs propagator. The relative simplicity of both $\delta\rho$ and the new coupling allows one to bypass the complications of the full $SU(2)\times U(1)$ Lagrangian. At the one-loop level, there are no diagrams involving the scalar x in the W-propagator corrections; therefore, the

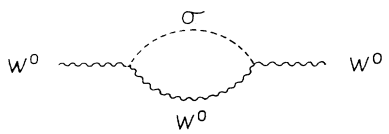

FIG. 2. One-loop correction to $\delta\rho$.

change in $\delta\rho$ due to the presence of the scalar, results entirely from the change in the Higgs propagator (2.7) itself. The contribution of each term in it can be calculated separately and yields the obvious replacement

$$\begin{aligned}\ln{m_H}^2\rightarrow&\alpha\ln{m_+}^2+(1-\alpha)\ln{m_-}^2\\&=\ln{m_-}^2+\alpha\ln\beta\ ,\end{aligned}\tag{4.1}$$

where

$$\beta={m_+}^2/{m_-}^2\ .\tag{4.2}$$

$\delta\rho$ is then found to be

$$\delta\rho=-\frac{3g^2}{64\pi^2}\tan^2\theta_w\left[\ln\frac{{m_-}^2}{{M_W}^2}+\alpha\ln\beta\right]\ ,\tag{4.3}$$

where θ_w is the weak mixing angle.

Note that in both limits $\lambda_2\rightarrow0$ and ${f_2}^2\rightarrow\infty$ the logarithmic term in (4.3) reduces to $\ln\lambda_1{f_1}^2$ as in the simple model. If ${f_2}^2\rightarrow0$, the logarithm becomes $\ln\lambda_3{f_1}^2$. Since the Higgs self-coupling is λ_3 as well, this is again the simple model. In the limits $\lambda_2\rightarrow0$ and ${f_2}^2\rightarrow0$ this is evident as x then decouples in the Lagrangian (2.2); in the limit ${f_2}^2\rightarrow\infty$ it is a consequence of the decoupling theorem. Equation (4.1) is not valid when $\lambda_2\rightarrow0$, since then ${m_-}^2\rightarrow0$, which violates the assumption that both scales are large compared to the W mass. For future reference note

$$\lim_{\lambda_2/\lambda_1\rightarrow\infty}\alpha=\frac{{f_1}^2}{{f_1}^2+{f_2}^2}\tag{4.4}$$

and

$$\lim_{{f_2}^2\rightarrow\infty}\alpha=0\ .\tag{4.5}$$

A graph of the deviation of (4.1) from $\ln\lambda_1{f_1}^2$ vs various values of ${f_2}^2/{f_1}^2$ is shown in Fig. 3(a); it is evident that the correction to $\delta\rho$ in the extended model can become arbitrarily large as $\beta\rightarrow\infty$, but this only happens if $\lambda_2/\lambda_1\rightarrow\infty$; β is bounded for finite values of λ_2/λ_1 [see Fig. 3(b)]. This may be understood as follows: If $\beta\rightarrow\infty$ for finite values of both λ_2/λ_1 and f_2, the theory would have a singularity, and if $f_2\rightarrow\infty$, then x decouples. The asymptotic behavior of the deviation from the standard model is

$$\begin{aligned}&\ln{m_-}^2+\alpha\ln\beta-\ln\lambda_1{f_1}^2\\&\xrightarrow{\lambda^2/\lambda_1\rightarrow\infty}\frac{1}{1+y}[\ln x+y\ln y+(1-y)\ln(1+y)]\ ,\end{aligned}\tag{4.6}$$

$$\xrightarrow{{f_2}^2/{f_1}^2\rightarrow\infty}\frac{\ln y}{y}\tag{4.7}$$

[cf. Figs. 3(a) and 3(b)], where

$$x=\lambda_2/\lambda_1\ ,\tag{4.8}$$

$$y={f_2}^2/{f_1}^2\ .\tag{4.9}$$

Note that the limit $y\rightarrow\infty$ is independent of x; this is also clear from Fig. 3(b). In the limit $x\rightarrow\infty$ the

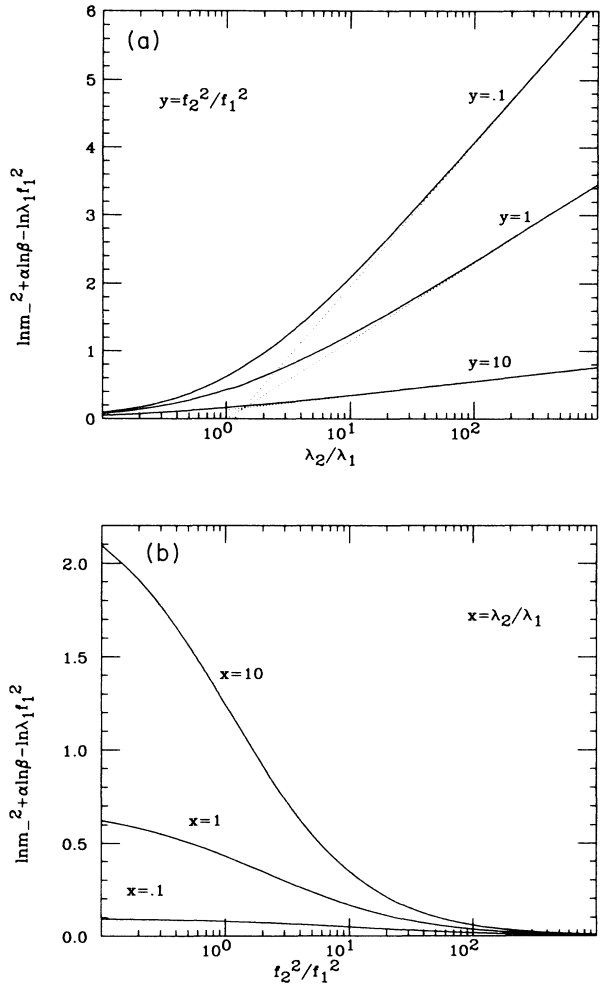

FIG. 3. (a) Logarithmic divergence vs x. (b) Logarithmic divergence vs y.

difference grows as the logarithm of the ratio of the scalar coupling constants. New effects will therefore be large if the two scales are widely separated.

V. CORRECTIONS TO THE $3W$ VERTEX

Only one diagram and its permutations contribute to the $3W$ vertex. It is shown in Fig. 4. Again, since it is logarithmically divergent and contains only one Higgs propagator, the result can be copied from the standard

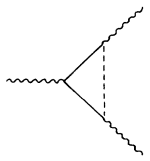

FIG. 4. One-loop correction to the $3W$ vertex.

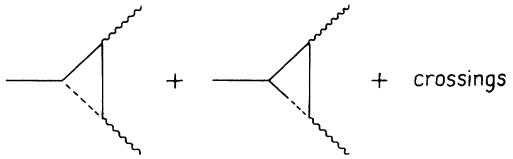

FIG. 5. One-loop correction to the $WW\phi$ vertex.

model with the replacement (4.1) (all momenta are incoming):

$$W^3=-\frac{1}{8}\frac{1}{16\pi^2}ig^3\epsilon_{abc}\left[\ln\frac{m_-^2}{M_W^2}+\alpha\ln\beta\right]$$
$$\times[(p-q)_\rho\delta_{\mu\nu}+(r-p)_\nu\delta_{\mu\rho}+(q-r)_\mu\delta_{\nu\rho}]\ . \quad (5.1)$$

The effective Lagrangian (2.14) yields, for the $3W$ vertex,

$$ig\epsilon_{abc}(\delta g+\tfrac{3}{2}Z_W+\alpha_3 g^2)$$
$$\times[(p-q)_\rho\delta_{\mu\nu}+(r-p)_\nu\delta_{\mu\rho}+(q-r)_\mu\delta_{\nu\rho}]\ . \quad (5.2)$$

Analogously to (5.1) one finds

$$Z_W=-\frac{1}{12}\frac{1}{16\pi^2}g^2\left[\ln\frac{m_-^2}{M_W^2}+\alpha\ln\beta\right]\ . \quad (5.3)$$

α_3 can easily be calculated from either one of the next two terms in the expansion of $\mathrm{Tr}(F_{\mu\nu}[V^\mu,V^\nu])$ because this is the only structure that has three-point vertices other than W^3. Figure 5 lists the diagrams which contribute to the $WW\phi$ vertex

$$WW\phi=-\frac{1}{12}\frac{1}{16\pi^2}\frac{g^2}{f_1}\epsilon_{abc}\left[\ln\frac{m_-^2}{M_W^2}+\alpha\ln\beta\right]$$
$$\times[p(q-r)\delta_{\nu\rho}+q_\nu q_\rho-r_\nu r_\rho]\ . \quad (5.4)$$

Comparison with (2.14) gives

$$\alpha_3=-\frac{1}{24}\frac{1}{16\pi^2}\left[\ln\frac{m_-^2}{M_W^2}+\alpha\ln\beta\right]\ . \quad (5.5)$$

This can be checked with the $W\phi\phi$ vertex (Fig. 6)

$$W\phi\phi=-\frac{1}{6}\frac{1}{16\pi^2}\frac{ig}{f_1^2}\left[\ln\frac{m_-^2}{M_W^2}+\alpha\ln\beta\right](r_\mu pq-q_\mu pr)\ , \quad (5.6)$$

from which again follows (5.5).

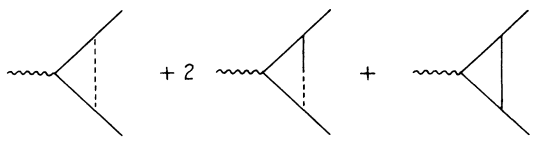

FIG. 6. One-loop correction to the $W\phi\phi$ vertex.

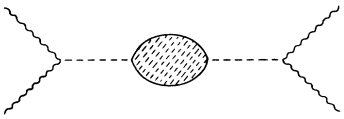

FIG. 7. Full single-Higgs-boson-exchange contribution to the $4W$ vertex.

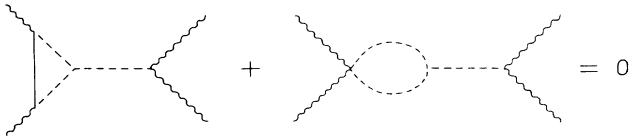

FIG. 8. Typical cancellation of diagrams in the $4W$ vertex.

In processes involving external vector bosons only, one cannot distinguish between a contribution of the form $\mathrm{Tr}(F_{\mu\nu}[V^\mu, V^\nu])$ and a renormalization of g. In order to understand the physical meaning of α_3 one introduces a coupling of the vector bosons to massless fermions for the purpose of fixing the corrections to the coupling constant g. This does not change any of the one-loop corrections considered in this paper, since the fermions are assumed to be massless. Because of gauge invariance, W bosons couple to fermions at the tree level with the same strength as to each other. Radiative corrections change this equality.

In fact, α_3 is a measure of this difference and one has[1,5]

$$g_{3W} - g_{W\bar{\psi}\psi} = a_3 g^3 \ . \tag{5.7}$$

Since the fermions are massless, they do not interact with the Higgs fields at the tree level and, therefore, the W-fermion coupling does not receive any one-loop corrections. One can thus define δg by requiring that the total one-loop contribution to $g_{W\bar{\psi}\psi}$ be zero. This immediately gives

$$\delta g + \tfrac{1}{2} Z_W = 0 \ . \tag{5.8}$$

As a consequence of Eq. (5.8) one finds from Eqs. (5.1)–(5.3) again that α_3 is given by Eq. (5.5). Note that the Higgs-boson mass dependence of the correction to the ρ parameter and the $3W$ vertex is the same. This shows that in processes in which the $4W$ vertex does not occur, one cannot distinguish between the model with an additional singlet and the simple standard model. This is not too surprising, since in both cases only diagrams with one Higgs propagator are involved. To find a process that might be sensitive to the presence of the extra particle one, therefore, has to study the $4W$ vertex. It provides the first example of multiple-Higgs-boson exchange.

VI. CORRECTIONS TO THE $4W$ VERTEX

It is convenient to classify the contributions to the $4W$ vertex as follows. There are three groups of diagrams: (i) those proportional to the tree-level vertex, in which there are only the counterterms and terms proportional to α_3; (ii) the completely symmetric diagrams, i.e., those proportional to

$$(\delta_{\mu\nu}\delta_{\rho\sigma} + \delta_{\mu\rho}\delta_{\nu\sigma} + \delta_{\mu\sigma}\delta_{\nu\rho})\delta_{ab}\delta_{cd} + \text{ permutations} \ ;$$

(iii) those proportional to

$$\delta_{\mu\nu}\delta_{\rho\sigma}\delta_{ab}\delta_{cd} + \text{ permutations} \ .$$

α_2 can be calculated directly, whereas α_1 contains the diagrams in Fig. 7 which depend on the Higgs counterterms. Therefore, a discussion of the renormalization of the Higgs sector precedes the evaluation of α_1. Several diagrams cancel, such as those in Fig. 8. The calculation can be checked by considering other processes; here the 4ϕ vertex was chosen because it is the only four-point function that does not involve W particles and is independent of whether or not the σ model is gauged.

A. Calculation of α_2

It follows from Table II that α_2 is determined by the diagrams in groups (i) and (ii) alone; its structure does not contain $\delta_{\mu\nu}\delta_{\rho\sigma}\delta_{ab}\delta_{cd}$. All counterterms have already been determined; (5.3), (5.5), and (5.8) give

$$\delta_{4W}(\text{counterterms}) = -\frac{1}{6}\frac{1}{16\pi^2} g^4 \left[\ln\frac{m_-^2}{M_W^2} + \alpha \ln\beta \right] (2\delta_{\mu\nu}\delta_{\rho\sigma} - \delta_{\mu\rho}\delta_{\nu\sigma} - \delta_{\mu\sigma}\delta_{\nu\rho})\delta_{ab}\delta_{cd} + \text{permutations} \ . \tag{6.1}$$

The box diagrams of Fig. 9 involve two Higgs propagators. A logarithmically divergent diagram which contains two propagators of the form (2.7), gives rise to the following deviation from the standard model:

$$\ln m_H^2 \to \alpha^2 \ln m_+^2 + 2\alpha(1-\alpha)\left[\ln m_-^2 + \frac{m_+^2}{m_+^2 - m_-^2} \ln\beta \right] + (1-\alpha)^2 \ln m_-^2$$

$$= \ln m_-^2 + \frac{\alpha}{m_+^2 - m_-^2}[2m_+^2 - \alpha(m_+^2 + m_-^2)] \ln\beta \ . \tag{6.2}$$

Figure 9 then gives

$$\delta_{4W}(\text{box graphs}) = -\frac{1}{12}\frac{1}{16\pi^2}g^4\left[\ln\frac{m_-^2}{M_W^2}+\frac{\alpha}{m_+^2-m_-^2}[2m_+^2-\alpha(m_+^2+m_-^2)]\ln\beta\right]$$
$$\times(\delta_{\mu\nu}\delta_{\rho\sigma}+\delta_{\mu\rho}\delta_{\nu\sigma}+\delta_{\mu\sigma}\delta_{\nu\rho})\delta_{ab}\delta_{cd}+\text{ permutations }. \tag{6.3}$$

The structure of α_2 is proportional to that combination of (i) and (ii) which does not contain $\delta_{\mu\nu}\delta_{\rho\sigma}\delta_{ab}\delta_{cd}$; therefore,

$$\alpha_2=\frac{1}{12}\frac{1}{16\pi^2}\left[\ln\frac{m_-^2}{M_W^2}-\frac{\alpha}{m_+^2-m_-^2}[2m_-^2-\alpha(m_+^2+m_-^2)]\ln\beta\right]. \tag{6.4}$$

This confirms that, in the Lagrangian (2.2), the corrections to the α_i depend on the number of Higgs propagators involved. To illustrate this further, note that one can form a combination of the α_i which is independent of the Higgs-boson mass in the standard model:

$$\alpha_2+2\alpha_3=\frac{1}{12}\frac{1}{16\pi^2}\alpha(1-\alpha)\frac{1+\beta}{1-\beta}\ln\beta\,. \tag{6.5}$$

Notice that if m_+^2 and m_-^2 are of the same order of magnitude, there is no essential difference with the standard model because (6.5) is bounded. However, if the mass ratio β becomes large, the difference with the standard model becomes large. This happens if $\lambda_2\gg\lambda_1$. An example is provided by $\lambda_2=\lambda_1^2$. Then one finds $\ln\beta\to\ln(m_-^2/M_W^2)$ and the relation with the nonlinear model, which gives $\alpha_2+2\alpha_3=O(1)$, is lost.

In the limit $\beta\to\infty$, (6.5) simplifies to

$$\alpha_2+2\alpha_3=-\frac{1}{12}\frac{1}{16\pi^2}\alpha(1-\alpha)\ln\beta\,. \tag{6.6}$$

A graph of (6.5) and (6.6) for $\alpha=\frac{1}{2}$ [this gives the maximum value for $\alpha(1-\alpha)$] is shown in Fig. 10.

Consider now the 4ϕ vertex in order to verify Eq. (6.4) analogously to Eq. (5.6) in Sec. V. For this, the 4ϕ vertex has to be expanded to $O(p^4)$. In almost all cases for every diagram with a Higgs propagator, there are also the same diagrams with mixed and x propagators. Therefore, the number of diagrams becomes very large, but only the box diagrams of Fig. 11 contribute to α_2; they were calculated in the limit $\beta\to\infty$ and give

$$\alpha_2=\frac{1}{12}\frac{1}{16\pi^2}\left[\ln\frac{m_-^2}{M_W^2}+\alpha^2\ln\beta\right]. \tag{6.7}$$

This agrees with (6.4).

B. Renormalization of the Higgs propagator

There are three propagators in the scalar part of the Lagrangian of the extended model; the three associated counterterms will be defined in an on-shell renormalization scheme. The cross section for W-W scattering due to one-Higgs-boson exchange in the extended model has two maxima and reaches zero between them [cf. Eq. (2.7)]. The maxima are at the poles of the Higgs propagator, $m_\pm^2$, and the zero is at $k^2=-m_0^2$, where, at the tree level,

$$m_0^2=\lambda_2 f_2^2\,. \tag{6.8}$$

The counterterms are defined such that the parameters in the Lagrangian describe the physical location of these three points; i.e., the sum of all one-loop corrections to the zero of the Higgs propagator, including the counterterms, vanishes at $k^2=-m_0^2$ and analogously for $m_\pm^2$. The parameters $m_\pm^2$ and m_0^2 are then the physical masses and the physical location of the zero of the cross section, respectively.

The quadratic part of the Lagrangian can be written as

$$\begin{aligned}\mathcal{L}_{\text{quadratic}} &= -\tfrac{1}{2}(\partial_\mu x)^2-\tfrac{1}{2}(\partial_\mu\sigma)^2-\tfrac{1}{2}(\partial_\mu\boldsymbol{\phi})^2\\ &\quad-\tfrac{1}{2}\lambda_3 f_1{}^2\sigma^2+\lambda_2 f_1 f_2 x\sigma-\tfrac{1}{2}\lambda_2 f_2{}^2 x^2\\ &= -\tfrac{1}{2}(x\quad\sigma)\Delta\begin{pmatrix}x\\ \sigma\end{pmatrix}\end{aligned} \tag{6.9}$$

with

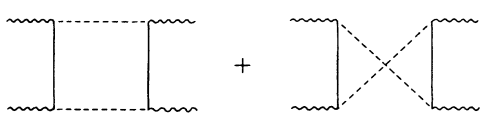

FIG. 9. Box diagrams contributing to the $4W$ vertex.

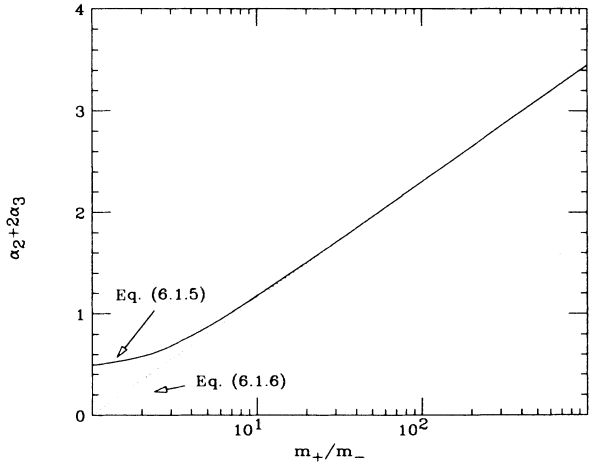

FIG. 10. Deviation of $\alpha_2+2\alpha_3$ from standard model.

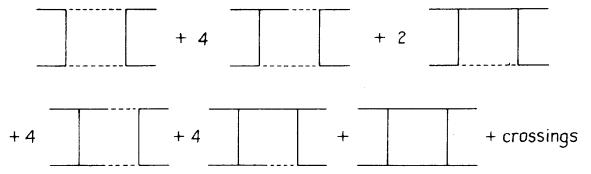

FIG. 11. Box diagrams contributing to α_2 in the 4ϕ vertex.

$$\Delta=\begin{bmatrix} k^2+\lambda_2 f_2{}^2 & -\lambda_2 f_1 f_2 \\ -\lambda_2 f_1 f_2 & k^2+\lambda_3 f_1{}^2 \end{bmatrix} . \tag{6.10}$$

The one-loop corrections to the inverse propagator, including the counterterms, can be written as

$$\Sigma=\begin{bmatrix} A & C \\ C & B \end{bmatrix} . \tag{6.11}$$

The corresponding diagrams are shown in Fig. 12.

Fields with vacuum expectation values have two types of mass counterterms: one is determined by the requirement that there be no tadpoles; the second type can still be fixed. To describe the effects of tadpole graphs one must allow for arbitrary shifts in the fields x and σ. An arbitrary shift in the x and σ fields effectively adds to the Lagrangian (2.2) a term

$$\mathcal{L}_{\text{tadpole}}=-c_1[f_1\sigma+\tfrac{1}{2}(\pi^2+\sigma^2)]-c_2 f_2 x . \tag{6.12}$$

The coefficients c_1 and c_2 are determined by the requirement that the vacuum expectation values of the x and σ fields vanish. The coefficient c_2 appears only in the term linear in x and has no physical consequence. The coefficient c_1, however, gives a contribution to the π and σ propagators. c_1 is given by the tadpole graphs of Fig. 13(a): $c_1=t_1+t_2$. Notice that t_1 cancels the contribution from the graph of Fig. 13(b), so that only t_2 appears among the diagrams of $B(k^2)$ in Fig. 12. The Ward identity $m_\pi{}^2=0$ provides a check on the value of c_1.

The poles of the propagator are given by the zeros of the eigenvalues of $\Delta-\Sigma$. The eigenvalues are

$$\lambda_+(k^2)=k^2+m_+{}^2-(1-\alpha)A(k^2) -\alpha B(k^2)+2\gamma C(k^2) , \tag{6.13}$$

$$\lambda_-(k^2)=k^2+m_-{}^2-\alpha A(k^2) -(1-\alpha)B(k^2)-2\gamma C(k^2) . \tag{6.14}$$

The location of the zero of the Higgs propagator is determined by

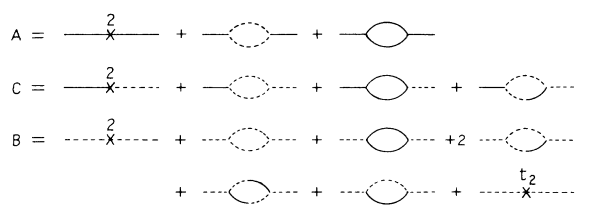

FIG. 12. One-loop Higgs propagator corrections.

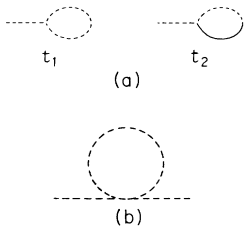

FIG. 13. (a) Tadpole graphs. (b) Graph which cancels counterterm.

$$\lambda_0(k^2)=\lambda_2 f_2{}^2-A(k^2) . \tag{6.15}$$

The counterterms in A, B, and C are now defined through

$$\lambda_\pm(-m_\pm{}^2)=0 \tag{6.16}$$

and

$$\lambda_0(-m_0{}^2)=\lambda_2 f_2{}^2 . \tag{6.17}$$

A, B, and C contain the three unknowns (cf. Fig. 12)

$$--\overset{2}{\times}--, \quad --\overset{2}{\times}\text{——}, \quad \text{and} \quad \text{——}\overset{2}{\times}\text{——}$$

and these are determined by Eqs. (6.16) and (6.17). One can then solve (6.16) and (6.17) for the counterterms. Writing

$$\lambda_\pm(k^2)=k^2+m_\pm{}^2[1+\delta_\pm(k^2)] ,$$

one finds

$$\begin{aligned} m_+{}^2\delta_+(k^2)=&(1-\alpha)[\bar{A}(-m_+{}^2)-\bar{A}(k^2)] \\ &+\alpha[\bar{B}(-m_+{}^2)-\bar{B}(k^2)] \\ &-2\gamma[\bar{C}(-m_+{}^2)-\bar{C}(k^2)] , \end{aligned} \tag{6.18}$$

$$\begin{aligned} m_-{}^2\delta_-(k^2)=&\alpha[\bar{A}(-m_-{}^2)-\bar{A}(k^2)] \\ &+(1-\alpha)[\bar{B}(-m_-{}^2)-\bar{B}(k^2)] \\ &+2\gamma[\bar{C}(-m_-{}^2)-\bar{C}(k^2)] , \end{aligned} \tag{6.19}$$

and

$$m_0{}^2\delta_0(k^2)=\bar{A}(-m_0{}^2)-\bar{A}(k^2) . \tag{6.20}$$

$\bar{A}$, $\bar{B}$, and $\bar{C}$ are here defined as A, B, and C in Eq. (6.11) but without the counterterms labeled with a 2 in Fig. 12. That is, $\bar{A}$, $\bar{B}$, and $\bar{C}$ are the corrections to the propagator (6.10) but without those counterterms that are fixed in Eqs. (6.16) and (6.17).

As stated before, $m_\pm{}^2$ and $m_0{}^2$ are the physical massive parameters in the theory; consequently, one has, by construction,

$$\delta_\pm(-m_\pm{}^2)=\delta_0(-m_0{}^2)=0 , \tag{6.21}$$

which is an alternative way of formulating the preceding statement. The diagram in Fig. 7 can now be calculated with the one-loop corrected Higgs propagator at $k^2=0$, which is

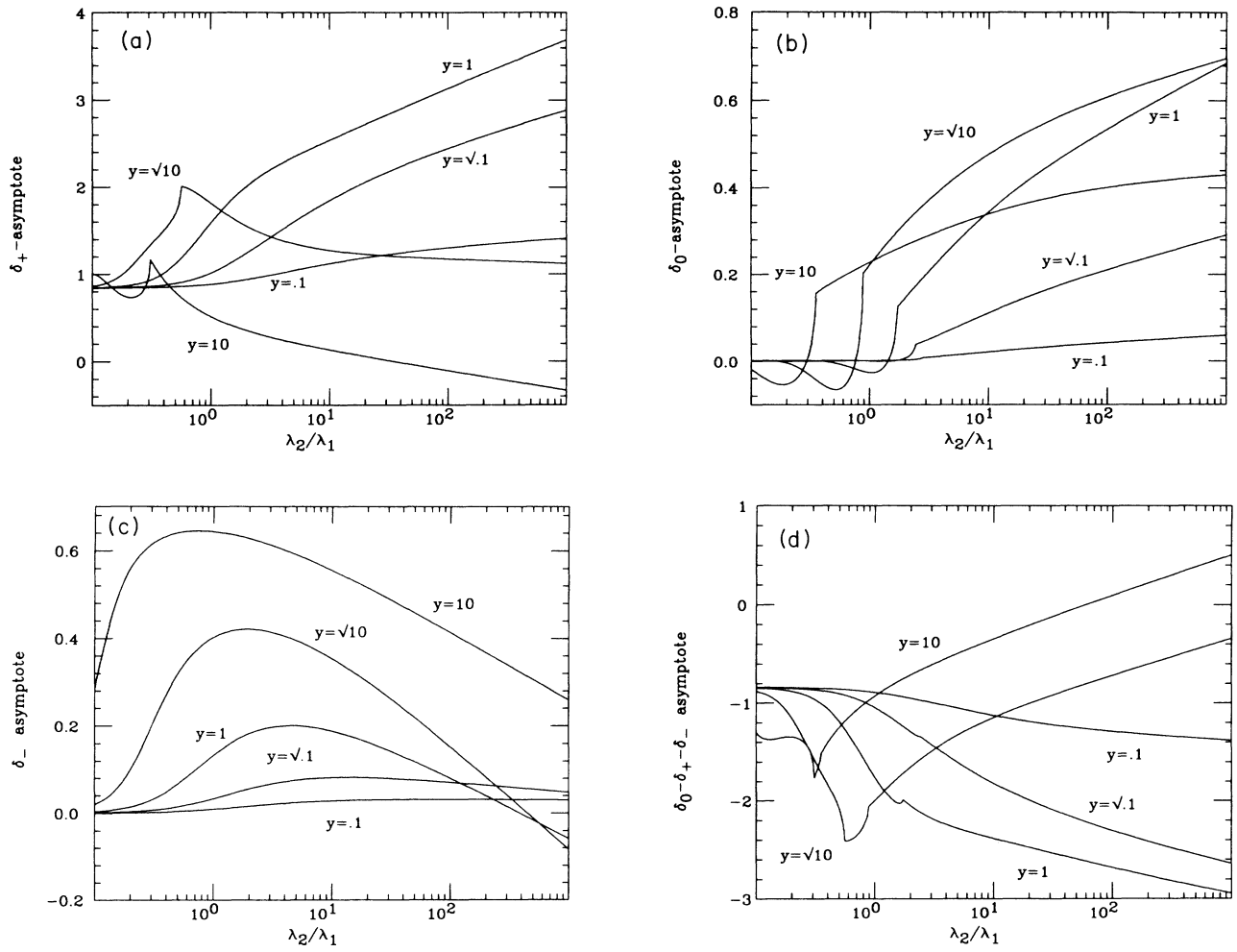

FIG. 14. (a) Deviation of δ_+ from asymptote. (b) Deviation of δ_0 from asymptote. (c) Deviation of δ_- from asymptote. (d) Deviation of δ_H from asymptote.

$$\sigma-\sigma(k^2=0)=\frac{\lambda_0(0)}{\lambda_+(0)\lambda_-(0)}=\frac{{m_0}^2}{{m_+}^2{m_-}^2}[1+\delta_0(0)-\delta_+(0)-\delta_-(0)]\,. \tag{6.22}$$

The calculation of the δ requires the evaluation of the integral

$$I_{ab}(p^2)=\int d^nk\frac{1}{(k^2+{m_a}^2)[(p+k)^2+{m_b}^2]} \tag{6.23}$$

for arbitrary values of p^2. Since it is not practical to quote the analytic expressions for the δ, they are presented graphically in Fig. 14. Only in the limit $\beta\to\infty$, simple expressions result. They are

$$\delta_0(0)=\tfrac{1}{2}\lambda_2\left[3\left[2-\ln\frac{{m_+}^2}{{M_W}^2}\right]-(1-\alpha)^2\ln\beta\right]+\tfrac{1}{2}\lambda_2\left[2(1-\alpha+\alpha^2)-2\alpha^2\left[\frac{3+\alpha}{1-\alpha}\right]^{1/2}\arctan\left[\frac{1-\alpha}{3+\alpha}\right]^{1/2}\right.$$
$$\left.+2\alpha^2\ln\alpha-(4-2\alpha+\alpha^2)\ln(1-\alpha)\right]+O(\lambda_1\ln\beta)\,, \tag{6.24}$$

$$\delta_+(0)=\frac{3}{2}\frac{\lambda_1\lambda_2{f_2}^2-\lambda_3{m_+}^2}{{m_+}^2-{m_-}^2}\left[\ln\frac{{m_+}^2}{{M_W}^2}-2\right]-\tfrac{1}{2}\lambda_2(1-\alpha)^2\ln\beta+\lambda_2\left[\frac{9}{2}\alpha^2\left[2-\frac{\pi}{\sqrt{3}}\right]+(1-\alpha)(1+3\alpha)\right]$$
$$-4\pi\sqrt{\lambda_1\lambda_2}\,\alpha^{3/2}(1-\alpha)^{3/2}+O(\lambda_1\ln\beta)\,, \tag{6.25}$$

$$\delta_-(0)=\frac{3}{2}\frac{\lambda_3 m_-{}^2-\lambda_1\lambda_2 f_2{}^2}{m_+{}^2-m_-{}^2}\left[\ln\frac{m_+{}^2}{M_W{}^2}-2\right]+\tfrac{1}{6}\lambda_2(1-\alpha)(3-\alpha)+O(\lambda_1\ln\beta)\ . \tag{6.26}$$

The deviation of the exact expressions for the δ's from the asymptotic formulas above is plotted in Figs. 14(a)–14(c). In these graphs the terms involving the factor $2-\ln(m_+{}^2/M_W{}^2)$, i.e., all diagrams containing π loops, have been omitted. This is because their contribution depends on a choice of scale which is independent of α and β. Also, terms of $O(M_W{}^2/m_-{}^2)$ have been neglected as we are only interested in the limit of large Higgs-boson mass. Figure 7 then becomes

$$\begin{aligned}\delta_{4W}(\text{Fig. 7})=\tfrac{1}{4}g^4\Bigg[&\frac{3}{2}\ln\frac{m_-{}^2}{M_W{}^2}+\frac{\lambda_2}{\lambda_1}\Bigg\{-\tfrac{9}{2}\alpha^2\left[2-\frac{\pi}{\sqrt{3}}\right]-\tfrac{1}{2}(4-2\alpha+\alpha^2)\ln(1-\alpha)\\&+\alpha^2\left[1-\left[\frac{3+\alpha}{1-\alpha}\right]^{1/2}\arctan\left[\frac{1-\alpha}{3+\alpha}\right]^{1/2}\right]+\alpha^2\ln\alpha-\tfrac{1}{6}(1-\alpha)(3+17\alpha)\Bigg\}\\&+4\pi\left[\frac{\lambda_2}{\lambda_1}\right]^{1/2}\alpha^{3/2}(1-\alpha)^{3/2}\Bigg]\delta_{\mu\nu}\delta_{\rho\sigma}\delta_{ab}\delta_{cd}+O(\lambda_1\ln\beta)+\text{ permutations}\ .\end{aligned} \tag{6.27}$$

$$\equiv\tfrac{1}{4}g^4\left[\frac{3}{2}\ln\frac{m_-{}^2}{M_W{}^2}+\delta_H\right]\delta_{\mu\nu}\delta_{\rho\sigma}\delta_{ab}\delta_{cd}+\text{ permutations}\ . \tag{6.28}$$

The deviation of δ_H from its asymptote is shown in Fig. 14(d). It is obvious from Fig. 14 that Eqs. (6.24)–(6.27) are correct to $O(\sqrt{\lambda_2/\lambda_1})$; the difference grows only logarithmically. Note finally that no tadpoles nor, in fact, any momentum-independent diagrams contribute to the expression (6.27) since they always cancel against the mass counterterms, as is already evident from Eqs. (6.18) and (6.19).

C. Calculation of α_1

The diagrams that give nonzero contributions to α_1 are listed in Figs. 7 and 15. All others cancel similarly to those in Figs. 1 and 8. The parameter α_1 is then found to be

$$\alpha_1=\frac{1}{24}\frac{1}{16\pi^2}\left[\ln\frac{m_-{}^2}{M_W{}^2}+3\delta_H+\frac{1}{2}\frac{\alpha}{m_+{}^2-m_-{}^2}[8m_-{}^2-6m_+{}^2-\alpha(m_+{}^2+m_-{}^2)]\ln\beta\right]\ , \tag{6.29}$$

where δ_H has been defined in the previous paragraph. In the limit $\beta\to\infty$, α_1 simplifies to

$$\alpha_1=\frac{1}{24}\frac{1}{16\pi^2}\left[\ln\frac{m_-{}^2}{M_W{}^2}+3\delta_H-\tfrac{1}{2}\alpha(6+\alpha)\ln\beta\right]\ . \tag{6.30}$$

Analogously to (6.6) there are now two more combinations of the α_i which vanish in the standard model, but are finite in the extended model: namely,

$$\alpha_1+\alpha_3=\frac{1}{24}\frac{1}{16\pi^2}[3\delta_H-\tfrac{1}{2}\alpha(8+\alpha)\ln\beta] \tag{6.31}$$

and

$$2\alpha_1-\alpha_2=\frac{1}{4}\frac{1}{16\pi^2}\left[\delta_H+\frac{1}{2}\frac{\alpha}{m_+{}^2-m_-{}^2}[4m_-{}^2-2m_+{}^2-\alpha(m_+{}^2+m_-{}^2)]\ln\beta\right]\ . \tag{6.32}$$

As before, the leading term in α_1 is independent of the Higgs-boson mass if $m_+{}^2\approx m_-{}^2$.

The structure constants α_i completely specify the effective Lagrangian at one loop. The calculation of α_1, therefore, concludes the determination of $\mathcal{L}_{\text{eff}}$. There is no obvious analog of the tree-level relation $g_{4W}=g_{3W}{}^2$ since the one-loop corrections to the $4W$ vertex are not proportional to the tree-level term; a new structure is generated. Even if δg_{4W} is defined as the correction to the tree-level vertex, its magnitude still depends on how the new structure is chosen. If one takes the completely symmetric term as the new structure, as was done in Ref. 5, one finds, for the $4W$ coupling,

$$W^4=g_{4W}(2\delta_{\mu\nu}\delta_{\rho\sigma}-\delta_{\mu\rho}\delta_{\nu\sigma}-\delta_{\mu\sigma}\delta_{\nu\rho})\delta_{ab}\delta_{cd}+g_{\text{new}}(\delta_{\mu\nu}\delta_{\rho\sigma}+\delta_{\mu\rho}\delta_{\nu\sigma}+\delta_{\mu\sigma}\delta_{\nu\rho})\delta_{ab}\delta_{cd}+\text{ permutations} \tag{6.33}$$

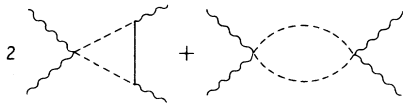

FIG. 15. Remaining contribution to α_1 in the $4W$ vertex.

with

$$g_{4W}=g_{3W}{}^2+\tfrac{1}{3}g^4(2\alpha_1-\alpha_2)\ , \tag{6.34}$$

$$g_{\text{new}}=\tfrac{1}{3}g^4(\alpha_1+\alpha_2)\ . \tag{6.35}$$

VII. CONCLUSION

We studied a model for the weak interactions in which the standard-model Higgs particle interacts strongly with a heavy singlet scalar. Because the masses of the particles are proportional to their coupling constants, the decoupling theorem does not apply and large effects may be present in the vector-boson interactions. The Higgs-boson-mass-dependent corrections to the effective Lagrangian of the vector bosons were calculated. The results were compared to the corrections in the standard model with a heavy Higgs particle but without the singlet. As long as the masses of the Higgs particle and the singlet are of the same order of magnitude, the effective Lagrangian contains only terms growing logarithmically with the Higgs-boson mass and the results are independent of the presence of the singlet scalar. The logarithmic effects remain related to the logarithmic divergences of the gauged nonlinear σ model.

If the ratio of the masses of the singlet and the Higgs scalar grows with the Higgs self-coupling, new corrections appear that are no longer related to the divergences of the nonlinear σ model. These corrections are only present if the Higgs-singlet coupling λ_2 increases more rapidly than the Higgs self-coupling λ_1, (i.e., $\lambda_2/\lambda_1\to\infty$ as $\lambda_1\to\infty$), so that there is a hierarchy of coupling strengths. In particular, there is a correction to the $4W$ vertex growing as $\lambda_2/\lambda_1\approx m_+{}^2/m_-{}^2$. Therefore, the model can describe massive vector bosons that have strong interactions among themselves and it makes a prediction of the structure of the strong-interaction vertex. It is remarkable that the $4W$ vertex can be stronger than indicated by the standard model without affecting the ρ parameter and the $3W$ vertex. The leading effects cannot be inferred any more from the underlying nonlinear σ model, but depend on the details of the scalar coupling. The assumed hierarchy of coupling constants is rather unnatural, but this might not be too much of a problem because the concept of naturalness is not well defined in strongly interacting theories. Such a hierarchy can perhaps arise in more complicated models such as technicolor, where the scalars are composite objects. In any case, it is consistent with experimental data which do not rule out strongly interacting W bosons. The situation is reminiscent of the standard model with a heavy top quark. Also, in this case, one has radiative corrections growing quadratically with the mass because the Yukawa coupling becomes strong. Large mass ratios can also be achieved through a hierarchy of vacuum expectation values, but in this case the corrections do not grow with the mass ratio.

ACKNOWLEDGMENTS

This work was supported in part by the U.S. Department of Energy. J.J.v.d.B. wishes to thank the University of Michigan for its hospitality.

[1]M. Veltman, Acta Phys. Pol. **B8**, 475 (1977).
[2]T. Appelquist and J. Carazzone, Phys. Rev. D **11**, 2856 (1975).
[3]R. Akhoury and Y. P. Yao, Phys. Rev. D **25**, 3361 (1982).
[4]M. Veltman, in *Proceedings of the Theoretical Advanced Study Institute in Elementary Particle Physics,* Ann Arbor, Michigan, 1984, edited by D. N. Williams (University of Michigan, Ann Arbor, MI, 1984).
[5]T. Appelquist and C. Bernard, Phys. D **22**, 200 (1980); **23**, 425 (1981).
[6]J. J. van der Bij and M. Veltman, Nucl. Phys. **B231**, 205 (1984); J. J. van der Bij, *ibid.* **B255**, 648 (1985).
[7]A. Longhitano, Phys. Rev. D **22**, 1166 (1980); Nucl. Phys. **B188**, 118 (1981).